*Desalination and Water Treatment*
www.deswater.com
12 (2009) 114–126
1944-3994 / 1944-3986 © 2009 Desalination Publications. All rights reserved.
doi: 10.5004/dwt.2009.945

# Synthesis and characterization of styrene-acrylonitrile copolymer blend ultrafiltration membranes

K.S. Radha[a], K.H. Shobana[a], D. Mohan[a]*, Y. Lakshmi Narayana[b]

[a]*Membrane Laboratory, Department of Chemical Engineering, A.C. College of Technology, Anna University Chennai, Chennai 600025, India*
*Tel. +91 (44) 2220 3530; Fax +91 (44) 2235 0299; email: mohantarun@yahoo.com*
[b]*Central Leather Research Institute, Chennai 600 025, India*

Received 19 July 2008; Accepted in revised form 13 July 2009

**ABSTRACT**

Polymeric blend new ultrafiltration membranes based on chemically and thermally stable styrene based copolymer were prepared by blending the styrene acrylonitrile copolymer (SAN) with cellulose acetate (CA) in N,N-dimethyl formamide (DMF) as polar solvent. Flat sheet asymmetric ultrafiltration CA/SAN blend membranes were fabricated using a suitable combination of solvent (DMF), non-solvent (water) both in the presence and absence of different additive concentrations, polyethylene glycol (PEG 600), by phase inversion technique. The performance of the new membrane material developed was investigated in terms of pure water flux, water content and membrane resistance. The surface and cross sectional morphologies of the membrane material were analyzed using scanning electron microscopy (SEM). Macromolecules such as pepsin, trypsin, egg albumin and bovine serum albumin were used as solutes in order to quantify the efficiency of protein separation of different blend membranes. The molecular weight cut-off (MWCO) and product rate efficiencies of the prepared membranes were also estimated. The effects of various polymer blend compositions and various additive concentrations on the above characteristics were analyzed in comparison with pure cellulose acetate membranes. The experimental results of the present work revealed that the CA/SAN blend membranes in the presence of additive have higher flux behavior than that of the membranes prepared from pure CA polymer.

*Keywords*: Cellulose acetate; Styrene acrylonitrile copolymer; Protein rejection; Molecular weight cut-off; Pore size

## 1. Introduction

The next generation of membrane materials and important trends in the separation field include synthesis of novel polymers and new polymeric blend membrane materials. The successful implementation of membrane technology has been due to the unique separation principle based on membranes. Continual development of new membrane material is crucial to sustain and expand the growing interest in this technology [1]. Technically mature membrane separation with a large growth potential in the next few years include especially UF and NF for concentration, fractionation and purification in the food, pharmaceutical, and other industries [2]. It often becomes imminent in the chemical and biochemical sciences to separate a component from a mixture, based on its molecular size of an individual component. The increasing complexity of chemical systems, in particular biochemical or biological systems, has required more sophisticated,

* Corresponding author.

*Presented at the Symposium on Emerging Trends in Separation Science and Technology (SESTEC-2008) March 12–14, 2008, University of Delhi, Delhi, India*

selective and efficient techniques to resolve/separate individual components [3]. In the last decade, ultrafiltration (UF) has become a standard procedure for the separation of macromolecular solutions. Separation of colloidal suspensions by ultrafiltration can be achieved by permselective membranes, which allow the passage of solvent and small solute molecules but retain macromolecules [4]. The separation of proteins by membranes was found to be advantageous because of the nondestructivity and limiting denaturation of proteins in the process [5]. The success of membrane technology lies in the membrane material. The proper selection of membrane material is critical to obtain the desired separation.

The first integrally skinned asymmetric cellulose acetate membranes were developed by Loeb and Sourirajan [6] and have been successfully employed in RO, UF processes and for separations in aqueous systems. However, application of CA membranes to the process which involves increasingly diversified macromolecular components, requires the modification of CA with a balanced hydrophilic–hydrophobic moiety [7]. In order to circumvent the inherent drawbacks of CA membranes such as poor thermal and chemical resistance, susceptibility to microbial attack, a very narrow pH range, poor chlorine resistance, lower flux, reduction in shelf life of membranes due to greater compaction phenomena, to bring about hydrophilic/hydrophobic balance in the membrane and to vary physico-chemical properties of the membrane, they have been prepared from multicomponent polymer mixtures/blends [8]. Synthesis of a polymer blend membrane was motivated by the necessity to superimpose requisite properties upon the basic transport properties of base polymer.

Styrene acrylonitrile (SAN) copolymer is an excellent engineering plastic which has some of the key properties similar to polysulfone [9]. Nowadays, the use of copolymer membranes has emerged as a new alternative and it has become of interest to many researchers. The SAN copolymers with 5–50% of acrylonitrile (hydrophilic component) in styrene (hydrophobic component) have greatly enhanced resistance to chemical attack, have good thermal stability, excellent resistance to biodegradation besides high rigidity and good surface hardness. A number of membranes using SAN were made for pervaporation [10,11] due to its solvent stability. Hence, SAN has been incorporated into CA to bring about desirable properties in the resultant blend membranes. This polymer pair exemplifies the use of polymer blend membrane composed of hydrophobic and hydrophilic polymers as those of polyacrylonitrile (PAN) and polyvinylchloride (PVC), cellulose acetate (CA) and polysulfone (PSf) in the literature [12–14]. The pore size of the membrane plays a significant role in its performance. The pore former plays a key role in enhancing the pore size of the asymmetric membranes [15]. The concentration of the pore former and its polarity have an influential effect on the membrane characterization [16]. Hence, an attempt was made to blend CA with SAN with DMF in the presence of pore former PEG 600, which was accepted as a suitable and appropriate additive in preparing membranes from the previous studies in our laboratory [17].

Pore statistics, molecular weight cut-off (MWCO) and the morphological studies are the structural properties of the membranes that are essential for the applications of membrane processes for the desired permeate quality [18]. It has been found that a broad variety of morphologically different polymeric membranes can be prepared by changing the parameters such as composition, concentrations of polymer, solvent and additive in the casting solutions [19,16].Thus, the effects of addition of SAN in the casting solution on the membrane properties were investigated by examining the UF membrane performances like compaction, pure water flux, water content, membrane resistance and protein rejection. The influence of performance of the membranes with the addition of different concentrations of PEG has also been investigated. Solute rejection method was used for determining pore statistics, MWCO, and the results are discussed. The morphology of the different membranes prepared with various blend compositions and additive concentrations used in the study was also studied using scanning electron microscopy.

## 2. Experimental

### 2.1. Materials

Commercial grade MYCEL cellulose acetate was procured from Mysore Acetate Chemicals Co. Ltd., India and styrene acrylonitrile copolymer (SAN) was obtained from BASF, India. Analar grade N, N′-dimethylformamide (DMF), sodium lauryl sulfate and other chemicals of analytical grade, used for membrane casting were purchased from Qualigens Fine Chemicals and SRL Chemicals Ltd. PEG 600 was procured from Merck (India) Ltd., and used as such as an additive for the whole study. Deionized and distilled water was used for all the studies.

### 2.2. Membrane preparation

The membranes were prepared by "phase inversion" technique [20]. The casting solution was prepared by dissolving CA in DMF solvent in a round bottom flask to which SAN copolymer was added and was subjected to constant stirring for 4 h at room temperature. The casting solution was kept in a dehumidifying chamber with a humidity of 35 ± 2% to remove air bubbles, and cast at room temperature by spreading them over a glass plate with the doctor blade to form a thin film membrane. The thickness of the membranes was maintained at 0.22 ± 0.02 mm and verified with a micrometer having a precision of 0.01 mm. The casting and gelation conditions were kept constant thoughout, since the thermodynamic conditions would

largely affect the morphology and performance of the resulting membranes [21]. The gelation bath consisting of 2.5% (v/v) DMF and 0.2% (wt basis) sodium dodecyl sulfate (SLS) in distilled water was prepared The former was added to reduce the rate of liquid–liquid demixing and macrovoid formation while the latter would reduce surface tension at the polymer–non-solvent interface. The solution after casting was exposed to atmosphere for 30 s for solvent evaporation and immediately immersed in the coagulation bath, maintained at 18°C. The membrane was kept undisturbed in the gelation bath for at least 1–3 h for complete precipitation and for leaching out of the solvent from the surface of the membrane during its formation. Later the membranes were removed and washed thoroughly with distilled water to remove excess DMF and surfactant and subsequently stored in 0.1 wt. % of formalin solution to avoid microbial attack [22]. The total fraction of solids in membrane formulation was held constant at 17.5 wt. % and the blend compositions of 95/5, 90/10, 85/15, /80/20, 75/25 wt. % (CA/SAN) of total polymer concentration in the casting solution were chosen for the preparation of CA/SAN blend membranes. The threshold limit of the SAN concentration was maintained to a maximum of 25 wt. % in CA polymer because beyond this concentration there was no compatibility between the polymers.

### 2.3. Experimental setup

The synthesized membranes were characterized using a batch type dead end cell (Ultrafiltration Cell–S76–400-Model, Spectrum, USA) with a diameter of 76 mm and effective membrane filtration area of 38.5 $cm^2$ fitted with Teflon coated magnetic paddle. The cell was connected to a nitrogen cylinder with the pressure control valve and a gauge through a feed reservoir.

### 2.4. UF characterization

The prepared CA/SAN membranes were characterized for compaction at a pressure of 414 kPa and the water flux was measured every 1 h for the duration of 10 min. Then the compacted membranes were used in UF experiments in the determination of pure water flux, water content and hydraulic resistance [17]. Further, the membrane morphology was also investigated using SEM.

#### 2.4.1. Compaction

The thoroughly washed membrane was cut into a desired shape and fitted in a UF kit. The distilled water was fed into the UF kit from the pressure reservoir and the initial water flux was taken after the pressurization at 414 kPa [17]. The membranes were compacted till the steady state was obtained. The compacted membranes were used in the subsequent UF experiments at 345 kPa.

#### 2.4.2. Pure water flux (PWF)

The compacted membranes were subjected to a differential system pressure of 345 kPa and the permeate was collected. The PWF was calculated using the equation

$$J_w = \frac{Q}{\Delta t \times A} \tag{1}$$

where $J_w$ is the pure water flux (l $m^{-2}h^{-1}$); $Q$ is the amount of permeates collected (l); $\Delta t$ is the sampling time (h) and $A$ is the membrane area ($m^2$).

#### 2.4.3. Water content

Water content of the membranes was obtained after soaking the membranes in water for 24 h, and then the membranes were weighed after mopping them with blotting paper. The wet membranes were placed in a vacuum drier at 75°C for 48 h and the dry weights were determined. The percentage water content was calculated based on the equation

$$\% \text{ water content} = \frac{\text{wet sample weight} - \text{dry sample weight}}{\text{wet sample weight}} \times 100 \tag{2}$$

#### 2.4.4. Membrane hydraulic resistance ($R_m$)

The membrane resistance is the resistance offered by the membrane to the feed flow. It is an indication of the tolerance of the membrane towards hydraulic pressure is calculated using the equation [23]:

$$R_m = \frac{\Delta P}{J_w} \tag{3}$$

To determine membrane hydraulic resistance ($R_m$), the pure water flux of the membranes was measured at different transmembrane pressures ($\Delta P$) viz., at 69, 138, 207, 276 and 345 kPa, after compaction. The resistance of the membrane, $R_m$, was evaluated from the slope obtained by plotting water flux vs. transmembrane pressure difference ($\Delta P$).

#### 2.4.5. Protein separation studies

##### 2.4.5.1. Molecular weight cutoff (MWCO)

Molecules having a molecular weight larger than the molecular weight cutoff (MWCO) of a membrane will not pass through the membrane. The MWCO of the membranes were determined using the different reference solutions. The solutes generally used are proteins which are considered to be spherical. Since the MWCO of a particular membrane corresponds to the molecular weight of the proteins having solute rejection beyond 80%, the MWCO of different membranes were determined from

the knowledge of percent rejection of different proteins by CA.

The protein rejection study was carried out using the protein solutions of different molecular weights such as trypsin (20 kDa), pepsin (35 kDa), egg albumin (45 kDa) and BSA (69 kDa). The experimental pressure was maintained at 345 kPa in nitrogen atmosphere for further study. The protein of the lowest molecular weight viz. trypsin was used first in order to reduce fouling of the membranes, followed by proteins of higher molecular weight. The protein solutions were prepared by dissolving 0.1 wt. % of it in phosphate buffer, which was used as standard feed solution. The pH of the buffer solution was maintained at 7.2, since any change in pH may lead to adsorptive fouling of the membrane surface [24]. Further, intermolecular forces between protein molecules and membranes will predominate and affect the efficiency of membranes if pH of the solution changes [25]. The concentration of the feed and the permeate collected was found using UV–Visible double beam spectrophotometer (Elica, SL164, Double Beam) at $\lambda_{max}$ = 280 nm. The permeate fluxes of all protein solutions as a function of PEG using membranes individually was determined by Eq. (1) and their % solute rejection was also found using the equation

$$\%SR = 1 - \frac{C_p}{C_f} \times 100 \tag{4}$$

where $C_p$ and $C_f$ are the concentrations of the solute in permeate and feed solutions.

*2.4.6. Pore statistics*

From the protein rejection studies, the average pore radius, surface porosity and pore density of the membrane were calculated. The average pore radius was found from % solute rejection and ε was calculated using the equation

$$\bar{R} = \frac{\bar{\alpha}}{\%SR} \times 100 \tag{5}$$

where $\bar{R}$ is the average pore radius (Å) of the membrane; $\bar{\alpha}$ is the average solute radius (Å) and is constant for each molecular weight. The average solute radius is known as "stoke radius" and the value of $\bar{\alpha}$ can be found from the plot between the solute radius and molecular weight of the solute given by Sarbolouki [26] which is shown in Table 7.

Assuming the membrane to be asymmetric skin type, the surface porosity of the membrane was found using the equation

$$\varepsilon = \frac{3\pi\eta_w J_{w1}}{R X \Delta P} \tag{6}$$

where ε is the surface porosity; $\eta_w$ is the velocity of the deionised water (g/cm s); $J_{w1}$ is the pure water flux (cm/s) and $\Delta P$ is the applied pressure (dyn/cm$^2$). From the known values of ε and $\bar{R}$ (in cm), the pore density in the membrane surface can be calculated using equation

$$n = \frac{\varepsilon}{\pi \times \bar{R}^2} \tag{7}$$

where $n$ is number of pores/cm$^2$.

*2.4.7. Morphological studies*

The top surface and the cross sectional view of the CA/SAN and pure CA membranes were analyzed using scanning electron microscopy. The membranes were cut into pieces of various sizes and mopped with filter paper. These pieces were immersed in liquid nitrogen for 20–30 s and frozen. The frozen bits of the membranes were broken and kept in a desiccator. The samples were mounted on sample holders called 'studs' and gold sputtered to provide electrical conductivity to very thin layers of those membranes. Then SEM micrographs of the samples were taken under very high vacuum and were analyzed.

## 3. Results and discussion

Extensive trials were carried out in our laboratory to get the best casting mixture giving desirable performance in terms of flux, water content and resistance from the prepared asymmetric membranes of CA/SAN blend with different compositions. The maximum possible blend composition was found to be 75/25 wt. % of CA/SAN in DMF, beyond which phase separation takes place (Table 1). The addition of pore former, PEG 600 was increased in 2.5% increments from 2.5 up to a maximum of 10 wt. % in the casting solution because beyond this concentration the miscibility decreased confirming the incompatibility of the two polymer components at higher PEG concentration.

### *3.1. Membrane compaction*

The membranes need a pre-pressure stabilization at a pressure higher than that operation limit in order to stabilize their mechanical properties regarding compressibility and stretch characteristics [27]. The fresh membranes were initially exposed to high pressure (414 kPa) for a period of 5–6 h till the membrane flux gradually declined to a steady state value asymptotically from a very high initial flux value. This may be due to the reduction in high porosity of fresh membranes when subjected to pressurization, which is otherwise mentioned as compaction of membrane pores. Similarly, at this constant operating pressure, the membrane flux of CA/SAN blend membranes at different compositions of polymer component and different concentrations of pore former were

Table 1
Composition and casting conditions of CA/SAN blend membranes

| Blend composition (%) | | PEG 600 | Solvent, DMF |
|---|---|---|---|
| CA | SAN | wt. % | wt. % |
| 100 | 0 | 0 | 82.5 |
| 95 | 5 | 0 | 82.5 |
| 90 | 10 | 0 | 82.5 |
| 85 | 15 | 0 | 82.5 |
| 80 | 20 | 0 | 82.5 |
| 75 | 25 | 0 | 82.5 |
| 100 | 0 | 2.5 | 80.0 |
| 95 | 5 | 2.5 | 80.0 |
| 90 | 10 | 2.5 | 80.0 |
| 85 | 15 | 2.5 | 80.0 |
| 80 | 20 | 2.5 | 80.0 |
| 75 | 25 | 2.5 | 80.0 |
| 100 | 0 | 5 | 77.5 |
| 95 | 5 | 5 | 77.5 |
| 90 | 10 | 5 | 77.5 |
| 85 | 15 | 5 | 77.5 |
| 80 | 20 | 5 | 77.5 |
| 75 | 25 | 5 | 77.5 |
| 100 | 0 | 7.5 | 75.0 |
| 95 | 5 | 7.5 | 75.0 |
| 90 | 10 | 7.5 | 75.0 |
| 85 | 15 | 7.5 | 75.0 |
| 80 | 20 | 7.5 | 75.0 |
| 75 | 25 | 7.5 | 75.0 |
| 100 | 0 | 10 | 72.5 |
| 95 | 5 | 10 | 72.5 |
| 90 | 10 | 10 | 72.5 |
| 85 | 15 | 10 | 72.5 |
| 80 | 20 | 10 | 72.5 |
| 75 | 25 | 10 | 72.5 |

Polymer, wt. % = 17.5

measured for every 1 h as shown in Table 2 and Fig. 1. From the table, it is observed that membranes prepared from pure CA with 17.5 wt. % casting solution showed a steady state of membrane flux at 14.0 $lm^{-2}h^{-1}$. In the CA/SAN blend membranes the steady state flux gradually increased from 15.6 to 32.7 $lm^{-2}h^{-1}$ with the increase in the composition of the SAN component. The comparatively higher flux in membranes with higher SAN content may be emphasized on the basis of partial miscibility of the blends leading to a larger polymer chain segmental gap between CA and SAN.

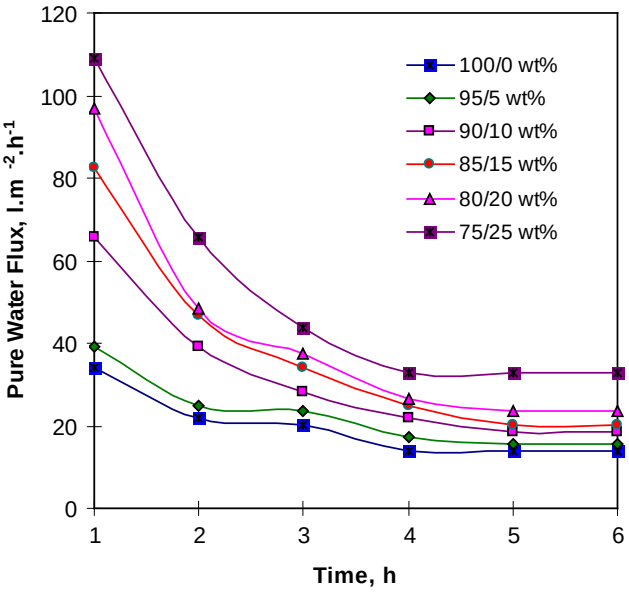


Fig. 1. Effect of compaction time on PWF of CA/SAN blend membranes.

### 3.2. *Pure water flux*

#### 3.2.1. *Effect of SAN composition:*

The water flux, an important and essential parameter for industrial process, is influenced by the composition of the membrane material or the conditions of operations [28]. The pressure stabilized membranes after compaction were subjected to the measurement of pure water flux at 345 kPa as shown in Table 3. The flux was measured under steady state flow [29]. The pure CA membrane showed the lowest value of pure water flux of 4.7 l $m^{-2}h^{-1}$ which may be due to the tight polymer matrix formed. Further, incorporation of SAN in the CA membrane up to 25 wt. % increased the pure water flux value to 23.4 l $m^{-2}h^{-1}$ which was due to the macrophase separation of the blend components that enhanced the pore size of the membrane [30].

#### 3.2.2. *Effect of PEG 600 concentration*

The increase in the concentration of additive and the pore former PEG 600 from 0 to 10 wt. % in pure CA membranes resulted in the increase in pure water flux from 4.7 to 54.6 $lm^{-2}h^{-1}$ as evidenced from Fig. 2. In the case of CA/SAN blend membranes, as the additive concentration was increased from 0 wt. % to 10 wt. % for the composition 95/5 wt. % and 75/25 wt. %, the magnitude of flux increased from 7.8 to 79.5 $lm^{-2}h^{-1}$ and 23.4 to 131.0 $lm^{-2}h^{-1}$ respectively. The increase in flux value was due to the incorporation of hydrophilic pore former PEG 600. This is attributed to leaching out of the non-solvent swelling agent, PEG 600, from the nascent membrane in the gelation bath. Hence, it is assumed that the additive was

Table 2
Effect of compaction time on PWF l $m^{-2}$ $h^{-1}$ at 414 kPa of CA/SAN blend membranes

| Blend composition (%) | | PEG 600 (wt. %) | Time (h) | | | | | |
|---|---|---|---|---|---|---|---|---|
| CA | SAN | | 0 | 1 | 2 | 3 | 4 | 5 |
| 100 | 0 | 0 | 34.3 | 24.9 | 23.4 | 14.0 | 14.0 | 14.0 |
| 95 | 5 | 0 | 39.0 | 21.8 | 20.3 | 17.2 | 15.6 | 15.6 |
| 90 | 10 | 0 | 65.5 | 39.0 | 28.1 | 21.8 | 19.5 | 19.5 |
| 85 | 15 | 0 | 82.6 | 46.8 | 34.3 | 24.9 | 20.3 | 20.3 |
| 80 | 20 | 0 | 96.7 | 48.3 | 37.4 | 23.4 | 23.4 | 23.4 |
| 75 | 25 | 0 | 109.1 | 65.5 | 43.7 | 32.7 | 32.7 | 32.7 |
| 100 | 0 | 2.5 | 93.6 | 70.2 | 51.5 | 39.0 | 39.0 | 39.0 |
| 95 | 5 | 2.5 | 152.8 | 98.2 | 74.8 | 49.9 | 43.7 | 43.7 |
| 90 | 10 | 2.5 | 171.5 | 109.1 | 79.5 | 51.5 | 51.5 | 51.5 |
| 85 | 15 | 2.5 | 184.0 | 118.5 | 93.6 | 56.1 | 56.1 | 56.1 |
| 80 | 20 | 2.5 | 201.1 | 152.8 | 106.0 | 68.6 | 57.7 | 57.7 |
| 75 | 25 | 2.5 | 210.5 | 155.9 | 123.2 | 74.8 | 74.8 | 74.8 |
| 100 | 0 | 5 | 121.6 | 101.4 | 65.5 | 48.3 | 48.3 | 48.3 |
| 95 | 5 | 5 | 171.5 | 116.9 | 84.2 | 67.0 | 67.0 | 67.0 |
| 90 | 10 | 5 | 210.5 | 127.9 | 93.6 | 81.1 | 81.1 | 81.1 |
| 85 | 15 | 5 | 249.5 | 148.1 | 112.3 | 85.8 | 85.8 | 85.8 |
| 80 | 20 | 5 | 280.7 | 163.7 | 132.5 | 109.1 | 95.1 | 95.1 |
| 75 | 25 | 5 | 304.1 | 179.3 | 145.0 | 124.7 | 112.3 | 112.3 |
| 100 | 0 | 7.5 | 149.7 | 123.2 | 101.4 | 74.8 | 74.8 | 74.8 |
| 95 | 5 | 7.5 | 241.7 | 126.3 | 96.7 | 79.5 | 79.5 | 79.5 |
| 90 | 10 | 7.5 | 265.1 | 145.0 | 107.6 | 87.3 | 87.3 | 87.3 |
| 85 | 15 | 7.5 | 304.1 | 160.6 | 145.0 | 110.7 | 110.7 | 110.7 |
| 80 | 20 | 7.5 | 319.6 | 198.0 | 155.9 | 131.0 | 123.2 | 123.2 |
| 75 | 25 | 7.5 | 382.0 | 218.3 | 199.6 | 148.1 | 135.7 | 135.7 |
| 100 | 0 | 10 | 187.1 | 143.5 | 132.5 | 81.1 | 81.1 | 81.1 |
| 95 | 5 | 10 | 249.5 | 138.8 | 107.6 | 93.6 | 93.6 | 93.6 |
| 90 | 10 | 10 | 288.5 | 155.9 | 113.8 | 101.4 | 101.4 | 101.4 |
| 85 | 15 | 10 | 311.9 | 194.9 | 149.7 | 131.0 | 112.3 | 112.3 |
| 80 | 20 | 10 | 343.0 | 215.2 | 165.3 | 143.5 | 132.5 | 132.5 |
| 75 | 25 | 10 | 405.4 | 241.7 | 212.1 | 159.0 | 151.2 | 151.2 |

Table 3
Effect of SAN composition on PWF of CA/SAN blend membranes with different additive concentrations

| Blend composition (%) | | PWF 1 $m^{-1}$ $h^{-1}$ at 345 kPa, PEG 600 concentration (wt. %) | | | | |
|---|---|---|---|---|---|---|
| CA | SAN | 0 | 2.5 | 5.0 | 7.5 | 10.0 |
| 100 | 0 | 4.7 | 15.6 | 24.9 | 35.9 | 54.6 |
| 95 | 5 | 7.8 | 31.2 | 49.9 | 67.0 | 79.5 |
| 90 | 10 | 14.0 | 35.9 | 68.6 | 85.8 | 92.0 |
| 85 | 15 | 15.6 | 39.0 | 73.3 | 93.6 | 101.4 |
| 80 | 20 | 18.7 | 43.7 | 84.2 | 102.9 | 110.7 |
| 75 | 25 | 23.4 | 57.7 | 98.2 | 107.6 | 131.0 |

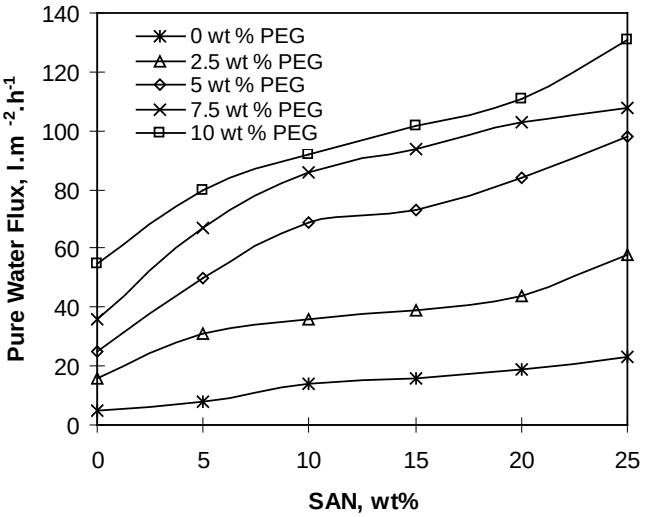


Fig. 2. Effect of SAN composition on PWF.

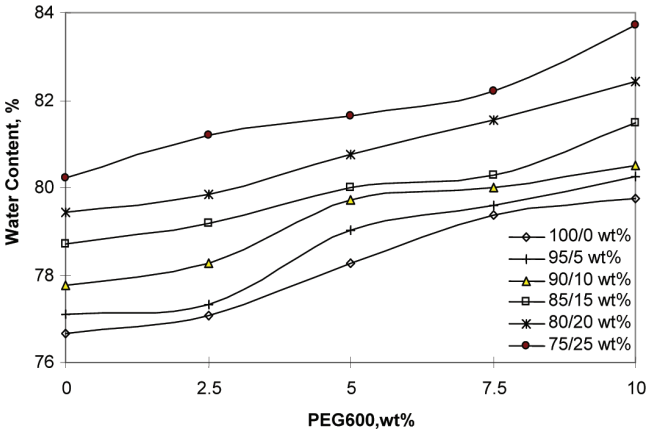


Fig. 3. Effect of PEG concentration on water content.

totally leached out in the gelation step, leaving the surface of the membranes with bigger pores and thereby increasing the PWF at higher PEG 600 concentration.

### 3.3. Water content

#### 3.3.1. Effect of SAN composition

Water content of the membrane is an indirect indication of hydrophilicity and the flux behavior of the membrane. The membranes were thoroughly washed with distilled water before subjecting them to percentage water content evaluation. The effect of SAN on CA membranes in terms of water content was studied and tabulated in Table 4. The water content of pure CA membranes was found to be 76.7%. With the increase in SAN content in the blend from 5 to 25 wt. % the percentage of water content was also found to increase linearly from 77.1 to 80.2%. This might be due to the increase in immiscibility between the two polymers CA and SAN which in turn decreased the adhesion properties between the polymeric chains. This led to an increase in void volume of the membrane by the increase in the size of super molecular polymer aggregates in the casting solution resulting in the formation of bigger pores.

#### 3.3.2. Effect of PEG 600 concentration

The water content of the membrane enhanced with the addition of PEG 600 to pure CA. Thus, at 0 wt. % PEG 600 the water content was found to be 76.7% and attained a maximum of 79.75% at 10 wt. % PEG 600. It is also evident from Table 4 and Fig. 3 that in the entire CA/SAN blend membranes with composition 95/5 to 75/25 wt. %, as the concentration of PEG 600 was increased from 0 to 10 wt. %, the water content also increased from 77.1 to 80.3 and from 80.2 to 83.7 respectively. The increasing trend may be due to the enhanced repulsive forces between the polymer segments which must have favoured the formation of macro voids which in turn has increased the pore size resulting in higher water content.

Table 4
Effect of SAN composition on water content of CA/SAN blend membranes with different additive concentrations

| Blend composition (%) | | Water content (%), PEG 600 concentration (wt. %) | | | | |
|---|---|---|---|---|---|---|
| CA | SAN | 0 | 2.5 | 5.0 | 7.5 | 10.0 |
| 100 | 0 | 76.7 | 77.1 | 78.3 | 79.4 | 79.7 |
| 95 | 5 | 77.1 | 77.3 | 79.0 | 79.6 | 80.2 |
| 90 | 10 | 77.8 | 78.3 | 79.7 | 80.0 | 80.5 |
| 85 | 15 | 78.7 | 79.2 | 80.0 | 80.3 | 81.5 |
| 80 | 20 | 79.4 | 79.8 | 80.8 | 81.6 | 82.4 |
| 75 | 25 | 80.2 | 81.2 | 81.6 | 82.2 | 83.7 |

### 3.4. Membrane hydraulic resistance

#### 3.4.1. Effect of SAN composition

Membrane hydraulic resistance is the intrinsic resistance of the membrane determined using pure water as the feed [31]. It is an indication of the tolerance of the membrane towards hydraulic pressure and is determined by subjecting the membranes to varied pressures (69–414 kPa) and measuring the PWF of the membranes. The linear proportionality of pure water flux to applied pressure can be directly associated with the transport resistance. This hydraulic resistance of the membranes was deduced from the inverse of the slope of the plot between transmembrane pressures and PWF. Since an increase in the operating pressure increased the driving force for permeation of the water, the PWF was observed to increase with the increase in transmembrane pressure. The pure water flux of the membranes measured at different transmembrane pressures with various concentrations was plotted and the results are shown in Figs. 4–7. From the slope of the above plots, the hydraulic resistance of the membranes was calculated (Table 5). The hydraulic resistance of pure CA membranes was found to be 34.1 kPa/lm$^{-2}$h$^{-1}$ and as the concentration of SAN increased from 5 to 25 wt. % in the blend, the hydraulic resistance decreased from 26.7 to12.7 kPa/lm$^{-2}$h$^{-1}$. This may be explained by the fact that an increase in the composition of SAN in the blend not only increased the amorphous nature of the membranes, but also enhanced the size of the pores to a greater extent due to an extended segmental gap between the polymer chains which led to the decrease in the membrane resistance [32].

#### 3.4.2. Effect of PEG 600 concentration

The effect of concentration of additive on membrane hydraulic resistance is shown in Figs. 4–7. As the concentration of the additive increased from 0 to 10 wt.%, the membrane resistance decreased from 34.1 to 5.1 kPa/lm$^{-2}$h$^{-1}$ in pure CA membranes. In the case of CA/SAN blend membranes of composition 95/5 and 75/25 wt.%, as the additive concentration in the casting

Table 5
Membrane hydraulic resistance of CA/SAN blend membranes with different additive concentrations

| Blend composition (%) | | $R_m$ (kPa/l m$^{-2}$h$^{-1}$), PEG 600 concentration (wt. %) | | | | |
|---|---|---|---|---|---|---|
| CA | SAN | 0 | 2.5 | 5.0 | 7.5 | 10.0 |
| 100 | 0 | 34.1 | 10.6 | 8.8 | 6.6 | 5.1 |
| 95 | 5 | 26.7 | 9.1 | 6.6 | 5.2 | 5.0 |
| 90 | 10 | 21.6 | 7.9 | 5.1 | 4.4 | 3.9 |
| 85 | 15 | 19.7 | 7.2 | 4.7 | 3.6 | 3.4 |
| 80 | 20 | 17.4 | 6.2 | 4.1 | 3.3 | 3.0 |
| 75 | 25 | 12.7 | 5.4 | 3.5 | 3.0 | 2.6 |

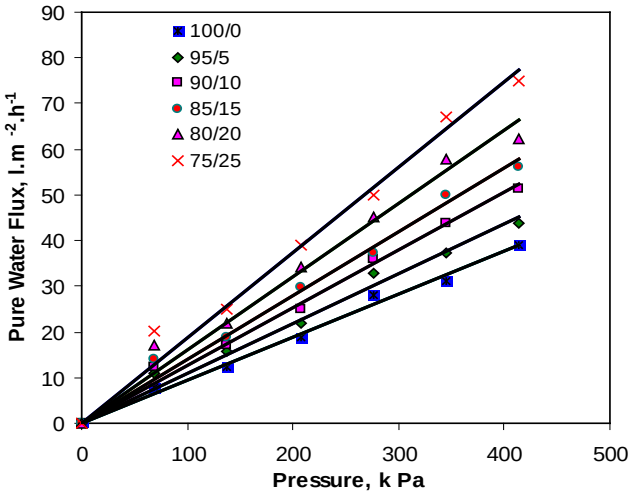


Fig. 4. Effect of transmembrane pressure on PWF of CA/SAN with 2.5 wt. % additive.

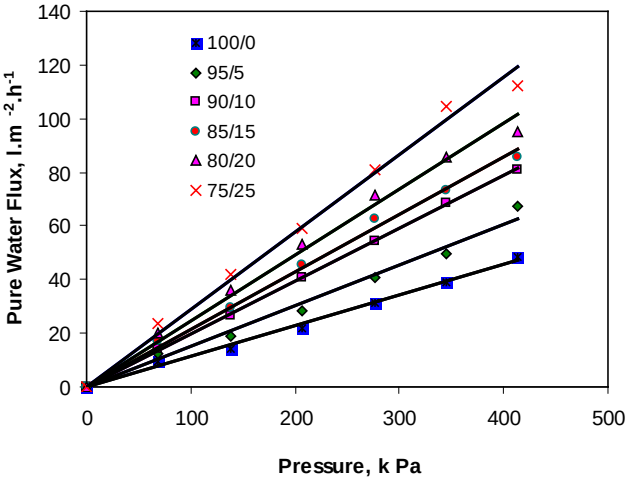


Fig. 5. Effect of transmembrane pressure on PWF of CA/SAN with 5 wt.% additive.

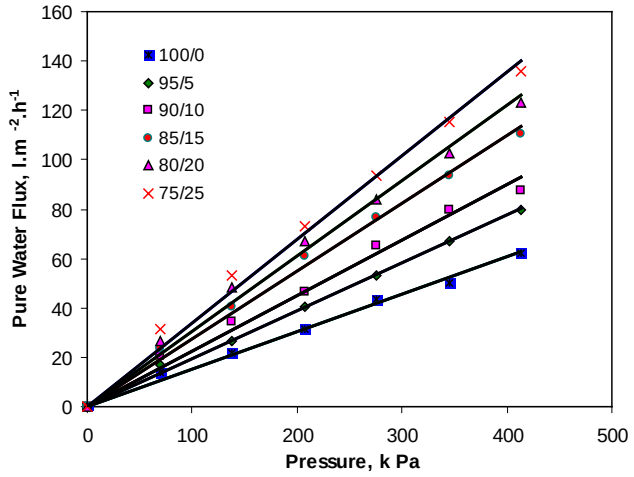


Fig. 6. Effect of transmembrane pressure on PWF of CA/SAN with 7.5 wt. % additive.

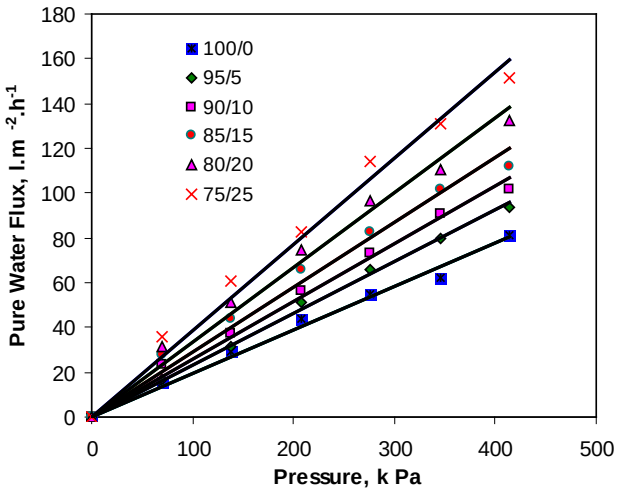


Fig. 7. Effect of trans-membrane pressure on PWF of CA/SAN with 10 wt. % additive.

solution was increased from 0 to 10 wt. %, hydraulic resistance decreased from 26.7 to 5.0 kPa/lm$^{-2}$h$^{-1}$ and from 12.7 to 2.6 kPa/lm$^{-2}$h$^{-1}$ respectively. The increase in additive concentration increased the pore size and reduced the resistance towards hydraulic pressure. This may be due to the fact that the addition of pore former in the casting solution resulted in the formation of macropores on the membrane surface due to thermodynamic instability, which enhanced precipitation and porous nature of the membrane [19].

### *3.5. Protein rejection studies and molecular weight cut-off (MWCO)*

#### *3.5.1. Effect of SAN composition*

Rejection measurements are often used to obtain information on the separation characteristics, and thus indirectly on the skin pores. The efficiency of protein rejection on blend composition is shown in Figs. 8 and 9. As it is observed, the solute rejection for CA membranes increased with the increase in the molecular weight of the proteins. The pure CA membrane in the absence of additive showed 90, 87, 83, and 80% rejection for BSA, EA, pepsin and trypsin, respectively. As the composition of SAN in the CA membrane increased to 25 wt. %, the rejection of protein molecules decreased to 82, 76, 70, and 67% for BSA, EA, pepsin and trypsin, respectively. This may be due to the fact that the higher SAN content created non-homogeneity between polymer matrices resulting in formation of pores in the membrane.

The permeate protein flux is the measure of product rate efficiency of the membrane for a given protein solution. As given in Figs. 10 and 11, pure CA exhibited a permeate flux of 2.5, 3.6, 4.0 and 4.2 l m$^{-2}$h$^{-1}$ for BSA, EA,

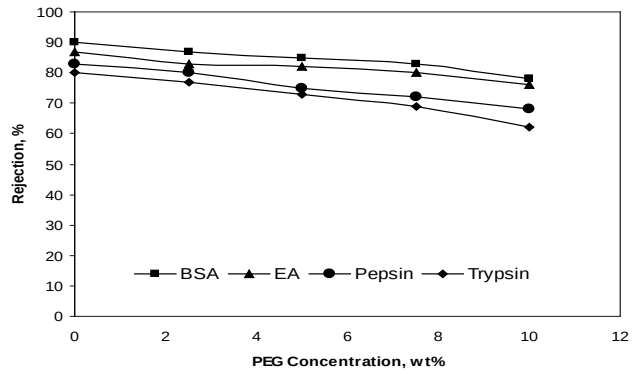


Fig. 8. Effect of PEG 600 on protein rejection in 100% CA membrane.

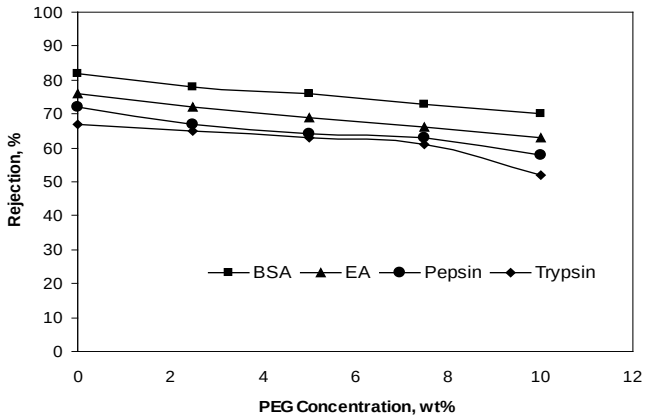


Fig. 9. Effect of PEG 600 on protein rejection in 75/25 wt% CA /SAN membrane.

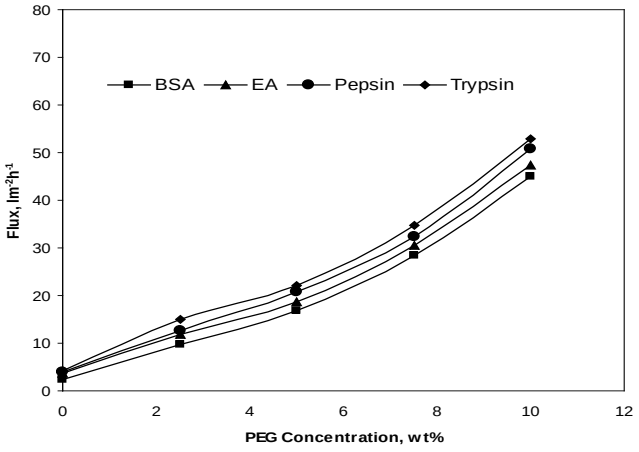


Fig. 10. Effect of PEG600 on protein flux in 100% CA membrane.

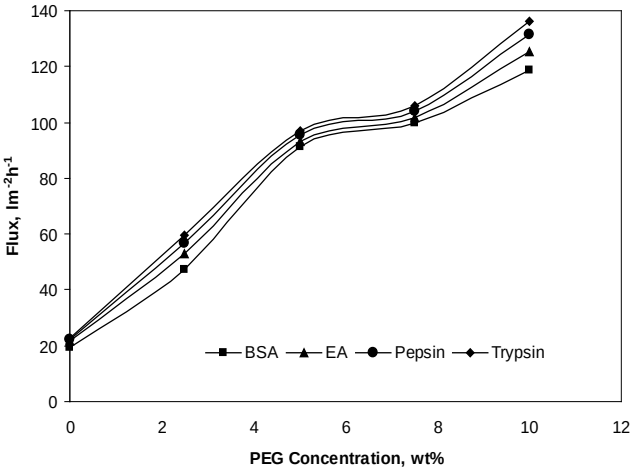


Fig. 11. Effect of PEG600 on protein flux in 75/25 wt. % CA/SAN membrane.

pepsin and trypsin, respectively. With the addition of SAN in the blend to 25 wt. %, the permeate flux increased to 19.3, 21.6, 22.1 and 22.9 l $m^{-2}h^{-1}$ for BSA, EA, pepsin and trypsin, respectively. This increase in flux with the increase in the addition of SAN to the blend was due to the increased immiscibility between CA and SAN components resulting in enhanced segmental gap leading to formation of bigger sized pores on the membrane surface. Thus trypsin showed a higher flux compared to other proteins due to its lower molecular weight and smaller solute radius.

Based on the rejection value of globular proteins and the procedure followed by Sarbolouki, the MWCO of CA/SAN membranes was determined and is reported in Table 6. The MWCO increased upon an increase in SAN

Table 6
Percentage rejection of proteins by CA/SAN blend membranes

| Blend composition (%) | | PEG 600 (wt. %) | PWF (l $m^{-2}h^{-1}$) | MWCO (kDa) | BSA (69 kDa) | EA (45 kDa) | Pepsin (35 kDa) | Trypsin (20 kDa) |
|---|---|---|---|---|---|---|---|---|
| CA | SAN | | | | | | | |
| 100 | 0 | 0 | 4.7 | 20 | 90 | 87 | 83 | 80 |
| 95 | 5 | 0 | 7.8 | 35 | 87 | 83 | 81 | 76 |
| 85 | 15 | 0 | 15.6 | 45 | 85 | 80 | 72 | 69 |
| 75 | 25 | 0 | 23.4 | 69 | 82 | 76 | 70 | 67 |
| 100 | 0 | 2.5 | 15.6 | 35 | 87 | 83 | 80 | 77 |
| 95 | 5 | 2.5 | 31.2 | 45 | 84 | 82 | 75 | 71 |
| 85 | 15 | 2.5 | 39.0 | 69 | 81 | 76 | 69 | 66 |
| 75 | 25 | 2.5 | 57.7 | >69 | 78 | 72 | 67 | 65 |
| 100 | 0 | 5 | 24.9 | 45 | 85 | 82 | 75 | 73 |
| 95 | 5 | 5 | 49.9 | 69 | 82 | 80 | 70 | 68 |
| 85 | 15 | 5 | 73.3 | >69 | 79 | 74 | 67 | 65 |
| 75 | 25 | 5 | 98.2 | >69 | 76 | 69 | 64 | 63 |
| 100 | 0 | 7.5 | 35.9 | 45 | 83 | 80 | 72 | 69 |
| 95 | 5 | 7.5 | 67.0 | 69 | 80 | 76 | 68 | 62 |
| 85 | 15 | 7.5 | 93.6 | >69 | 75 | 70 | 65 | 64 |
| 75 | 25 | 7.5 | 107.6 | >69 | 73 | 66 | 63 | 61 |
| 100 | 0 | 10 | 54.6 | >69 | 78 | 76 | 68 | 62 |
| 95 | 5 | 10 | 79.5 | >69 | 76 | 73 | 64 | 59 |
| 85 | 15 | 10 | 101.4 | >69 | 71 | 67 | 60 | 54 |
| 75 | 25 | 10 | 131.0 | >69 | 70 | 63 | 58 | 52 |

content in the blend. This may be due to formation of a segmental gap as a result of partial phase separation upon proportionately increasing concentration of SAN.

*3.5.2. Effect of PEG 600 concentration*

With the increase in additive concentration, the rejection was found to decrease as shown in Figs. 8 and 9. As the concentration of the additive increased from 0 to 10 wt. %, the rejection of protein molecules decreased from 90 to 78%, from 87 to 76%, from 83 to 68%, and from 80 to 62% for BSA, EA, pepsin and trypsin, respectively, in pure CA membranes. This may probably be due to the increase in the size of the pores with the increase in additive concentration which was due to leaching out of the additive during gelation due to its water soluble nature.

The presence of additive in the casting solution has a significant effect on protein flux of resulting membranes as seen in Figs. 10 and 11. When the PEG 600 concentration was increased to 10 wt. % in pure CA membranes, the permeate flux was increased to 45.1, 47.3, 50.7, and 52.9 l $m^{-2}h^{-1}$ for BSA, EA, pepsin and trypsin, respectively. The increasing trend in the permeate flux indicates the increase in the pore size resulting from higher additive concentrations of PEG 600 from 0 to 10 wt. %.

Similarly, an increase in PEG 600 content from 0 to 10 wt. % resulted in the increase in MWCO as reported in Table 6, which may be due to fast rate of leachability of PEG 600 during the gelation process, which left a large pore on the membrane surface.

*3.6. Pore statistics*

The pore statistics include average pore radius (Å) and surface porosity (ε) of the membrane. As it is observed from Table 7, the values of both the parameters showed an increasing trend with the increase in SAN content from 0 to 25 wt. % in the blend membrane. This may be due to the amorphous nature of the blend and increased immiscibility of CA and SAN in the polymer matrix leading to an enhanced segmental gap between the polymer chains.

*3.7. Morphological studies*

The scanning electron microscopy images were taken for the pure CA membranes and the CA/SAN blend membranes in the presence of pore former, PEG. The SEM micrographs of the top surface and cross section of the membranes prepared from 100% CA in different additive concentrations are shown in Figs. 12a–f. It is evident from

Table 7
Pore statistics of CA/SAN blend membranes

| Blend composition (%) | | Average membrane radius $\bar{R}$ (Å) | Surface porosity $\varepsilon \times 10^{-5}$ |
|---|---|---|---|
| CA | SAN | | |
| 100 | 0 | 26.88 | 1.73 |
| 95 | 5 | 35.63 | 2.16 |
| 85 | 15 | 41.25 | 3.73 |
| 75 | 25 | 56.25 | 4.46 |

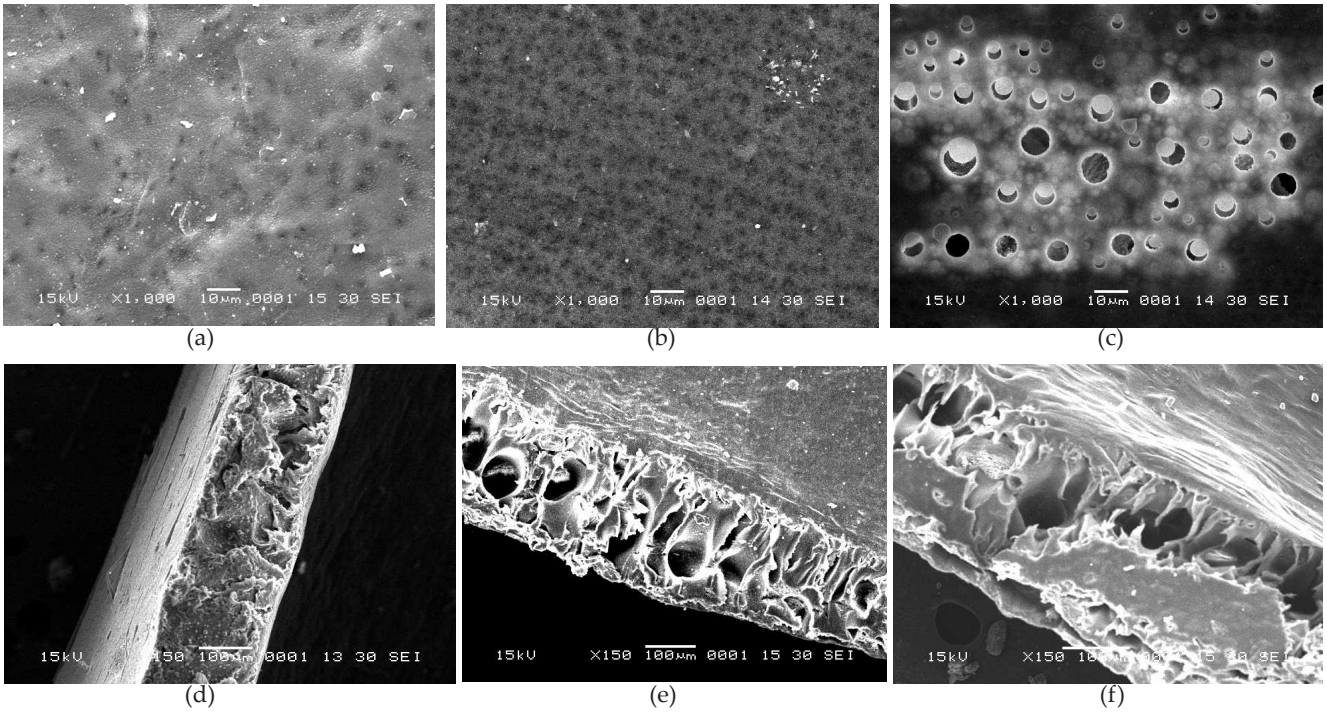


(a) (b) (c)

(d) (e) (f)

Fig. 12. SEM micrographs of 100% CA membranes with different concentrations of PEG. Top surface (1000×): a) 2.5 wt. %; b) 5 wt. %; c) 7.5 wt. % cross section (150×); d) 2.5 wt. %; e)5 wt. %; f) 7.5 wt. %.

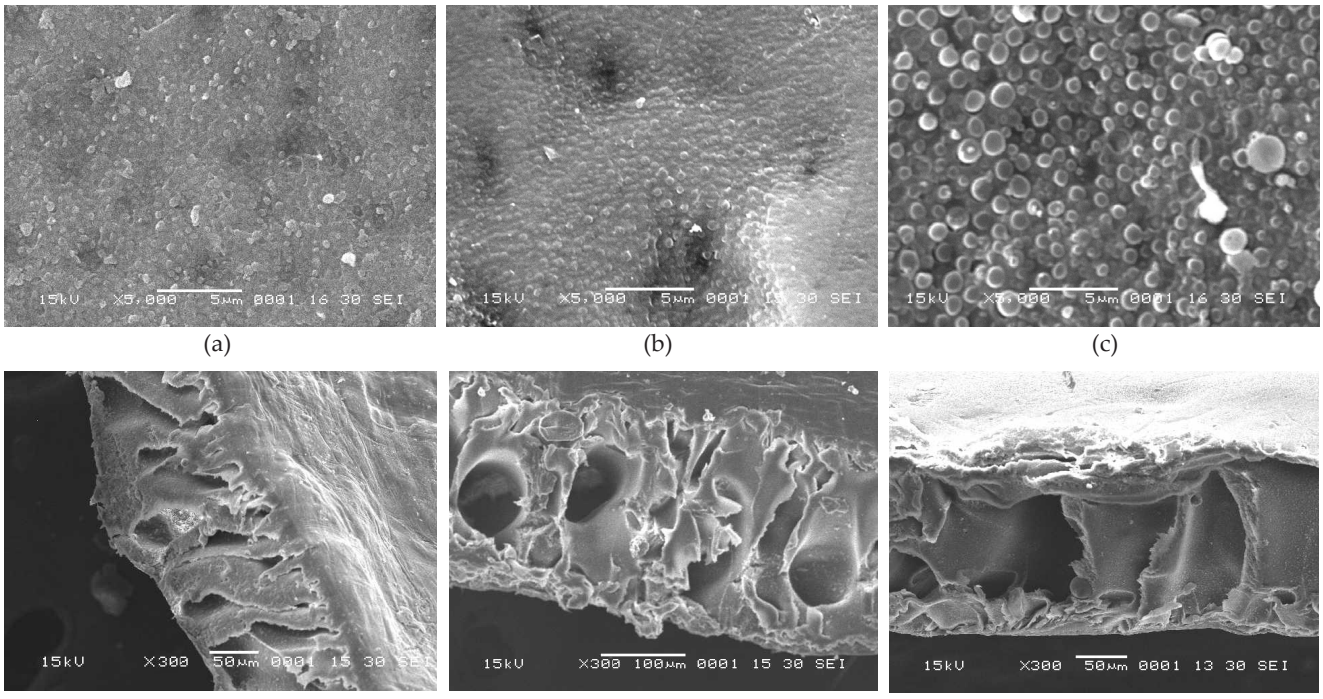


Fig. 13. SEM micrographs of CA/SAN (75/25) membranes with different concentrations of PEG. Top surface (5000×): a) 2.5 wt.% b) 5 wt. %; c) 7.5 wt. % cross section (300×); d) 2.5 wt. % ;e) 5 wt. %; f) 7.5 wt. %.

the figures that upon increasing the additive concentration from 2.5 to 7.5 wt. %, the pore sizes and finger like voids also increased. This confirms the concept of leaching out of additive during gelation. This type of morphological results from SEM confirms the effect of additive on PWF, water content and hydraulic resistance. Similarly the CA/SAN blend membranes with various additive concentrations has a good correlation with the membrane morphology. Figs. 13a–f exhibit the top surface and cross sectional view of the CA/SAN blend membranes of 75/25 wt. % composition with 2.5–7.5 wt. % of additive concentrations. As the PEG concentration was increased in the casting dope, the porosity also increased linearly which could be observed from the scanned skin surface of the respective membranes. It is evidenced from the figures that as the SAN content in the blend was increased to 25 wt. %, the number of pores also increased. Further, the morphological studies confirmed our experimental trends in the case of the blend membranes.

## 4. Conclusion

In this investigation, a novel type of styrene based copolymer (SAN) blend membrane material was developed using cellulose acetate as the base polymer. These blend membranes with different compositions of CA/SAN and various concentrations of additive (PEG 600) showed enhanced ultrafiltration membrane characteristics, such as higher water content and lower $R_m$ values coupled with higher pure water flux in comparison with pure cellulose acetate membranes. The extent of compatibility of SAN with CA under room conditions was 75/25 wt. % of CA/SAN and the maximum additive compatibility was found to be 10 wt. %. The blend composition and presence of various amounts of additive are the important factors in changing the PWF, water content and membrane resistance of the blend membranes. Such novel polymeric blend membranes based on CA and SAN have been effectively used for the aqueous separation of proteins such as BSA, EA, pepsin and trypsin by ultrafiltration. The separation of proteins was carried out to determine the MWCO values. The separation of BSA was comparatively higher, in view of its higher molecular weight (69 kDa). Further SEM analysis showed that incorporation of additive in the blend system altered the structural properties and morphology of the membranes to a greater extent.

## Acknowledgement

The authors express their gratitude to BASF, Ltd. for the gift sample of styrene acrylonitrile used for the preparation of blend membranes.

## References


[1] M.M. Dal-Cin, C.M. Tam, M.D. Guiner and T.A. Tweddle, J. Appl. Polymer Sci., 54 (1994) 783.
[2] R.W. Baker, Membrane Technology and Applications, 2nd ed., Chichester, Wiley, 2004.
[3] A. Saxena and V.K. Shahi, J. Membr. Sci., 299 (2007) 211–221.
[4] G. Arthanareeswaran, P. Thanikaivelan, J. Abdoul Rabuime, M. Rajenthiren and D. Mohan, Separ. Purif. Technol., 55 (2007) 8–15.
[5] A. Nagendran, D. Lawrence Arockiasamy and D. Mohan, Mater. Manufact. Processes, 23 (2008) 311–319.
[6] S. Loeb and S. Sourirajan, Adv. Chem. Ser., 38 (1963) 117.
[7] W.W.Y. Lau and Y. Jiang, Polymer Intern., 33 (1994) 413.
[8] M. Sivakumar, D. Mohan and R. Rangarajan, Polymer Intern., 47 (1998) 311.
[9] N.V. Desai, R. Rangarajan, A.V. Rao, D.K. Garg, B.V. Ankleshwaria and M.H. Mehta, J. Membr. Sci., 71 (1992) 201.
[10] S. Mandal and V.G. Pangarkar, J. Membr. Sci., 209 (2002) 53–66.
[11] S.K. Ray, S.B. Sawant, J.B. Joshi and V.G. Pangarkar, Ind. Eng. Chem. Res., 36 (1997) 5265–5276.
[12] F. Tomohiro, N. Yasuhiko and N. Yasuki, Japan Kokai, Tokyo Hoho Jp., 6 (1994) 256, 656.
[13] R. Malaisamy, R. Mahendran and D. Mohan, J. Appl. Polymer Sci., 84 (2002) 430.
[14] R. Mahendran, R. Malaisamy, G. Arthanareeswaran and D. Mohan, J. Appl. Polymer Sci., 92 (2004) 3659.
[15] M. Sivakumar D. Mohan and R. Rangarajan, J. Membr. Sci., 268 (2006) 208–219.
[16] T.D. Nguyen, T. Matsuura and S. Sourirajan, Chem. Eng. Commun., 54 (1987) 17.
[17] M. Sivakumar, R. Malaisamy, C.J. Sajitha, D. Mohan, V. Mohan and R. Rangarajan, J. Membr. Sci., 169 (2000) 215.
[18] L. Zeman and M. Wales, Separ. Sci. Technol., 16 (1981) 275.
[19] C. Stropnik, L. Germic and B. Zerjal, J. Appl. Polymer Sci., 61 (1996)1821–1830.
[20] P.S.T. Machado, A.C. Habert and C.P. Borges, J. Membr. Sci., 155 (1999) 171.
[21] C. Barth, M.C. Gonclaves, A.T.N. Pires, J. Roeder and B.A. Wolf, J. Membr. Sci., 169 (2000) 287.
[22] M. Sivakumar, A.K. Mohanasundaram, D. Mohan, K. Balu and R. Rangarajan, J. Appl. Polymer Sci., 67 (1998) 1939–1946.
[23] Y.Q. Wang, Y.L. Su, Q. Sun, X.L. Ma and Z.Y. Jiang, J. Membr. Sci., 286 (2006) 228–236.
[24] J. Brinck, A.S. Jonsson, B. Jonsson and J. Lindau, J. Membr. Sci., 164 (2000) 187–194.
[25] J.A. Koehler, M. Ulbricht and G. Belfort, Langmuir, 12 (1997) 4162.
[26] M.N. Sarbolouki, Separ. Purif. Technol., 17 (1982) 228–386.
[27] M. Joshi, A.K. Mukherjee and B.D. Thakur, J. Membr. Sci., 189 (2001) 23–40.
[28] B. Kunst and Z. Vajnaht, J. Appl. Polymer Sci., 21 (1977) 2505–2514.
[29] N.I. Osada, Membrane Science and Technology, Marcel Dekker, New York, 1992.
[30] H. Yasuda and J.T. Tsai, J. Appl. Polymer Sci., 18 (1974) 805–819.
[31] M. Cheryan, Ultrafiltration Handbook, Technomic Publications, Lancaster, 1986.
[32] R.E. Kesting, Synthetic Polymeric Membranes, Wiley Interscience, New York, 1985.